Complete and Consistent All-Region Body-Referenced Capacitance Model Based on Symmetric Linearization

Colin McAndrew
Freescale Semiconductor
Tempe, AZ

Abstract

The book (*Operation and Modeling of the MOS Transistor, 3rd Edition,* by Yannis Tsividis and Colin McAndrew, Oxford University Press, 2011) presents a complete all-region I_{DS} model based on the bulk charge[*] model (4.3.12) ($Q_B^{'} = -\gamma C_{ox}^{'} \sqrt{\psi_s}$) and in Chap. 6 provides charge models, but does not present a complete and numerically stable charge model valid in all regions of operations; the details were considered too complex for the book and potentially distracting by providing too much mathematical detail which could detract from understanding of basic modeling approaches and physical device operation. Complete and consistent all-region dc and charge models, based on the symmetric linearization procedure, were provided in supplementary material on the books' website (www.oup.com/us/tsividis_mcandrew). With the advent of Verilog-A, dc and charge models (and noise, geometry scaling, and temperature models) are all that is required to implement a model for circuit simulation; the necessary derivatives, i.e. capacitances and conductances, are automatically generated from the Verilog-A code by Verilog-A compilers. However, it can sometimes be useful to have expressions for the capacitances themselves. Capacitances expressions for the symmetric linearization charge model are provided here.

[*] As in the book, we use the term "charge" rather than "charge per unit area" for simplicity. The fact that we are talking about charges *per unit area* will be clear from the primes used in the symbols for these quantities. The same applies to capacitances.

Copyright © 2011 by Oxford University Press

Introduction

Complete charge expressions for the symmetric linearization all-region model [1] are derived in the supplementary material on the books' website (www.oup.com/us/tsividis_mcandrew) and are repeated below for convenience:

(1) $$Q_G = LWC_{ox}^{'}\left(V_{GB} - V_{FB} - \psi_{sm} + \frac{\Delta\psi_s^2}{12H}\right) - Q_o$$

(2) $$Q_B = -\operatorname{sgn}(\psi_{sm})LWC_{ox}^{'}\left[\gamma\sqrt{\psi_{am}} - \frac{(\alpha_m - 1)\Delta\psi_s^2}{12H}\right]$$

(3) $$Q_I = Q_S + Q_D = -LWC_{ox}^{'}\left(\psi_{im} + \frac{\alpha_m\Delta\psi_s^2}{12H}\right)$$

(4) $$Q_S = -\frac{LWC_{ox}^{'}}{2}\left[\psi_{im} + \frac{\alpha_m\Delta\psi_s}{6}\left(1 + \frac{\Delta\psi_s}{2H} - \frac{\Delta\psi_s^2}{20H^2}\right)\right]$$

(5) $$Q_D = -\frac{LWC_{ox}^{'}}{2}\left[\psi_{im} - \frac{\alpha_m\Delta\psi_s}{6}\left(1 - \frac{\Delta\psi_s}{2H} - \frac{\Delta\psi_s^2}{20H^2}\right)\right]$$

where the midpoint surface potential is

(6) $$\psi_{sm} = \frac{\psi_{s0} + \psi_{sL}}{2},$$

the potential that characterizes the normalized non-inversion silicon charge per unit area at the midpoint surface potential is

(7) $$\psi_{am} = \phi_t e^{-\psi_{sm}/\phi_t} + \psi_{sm} - \phi_t,$$

the potential that characterizes the normalized inversion layer charge per unit area at the midpoint surface potential is

(8) $$\psi_{im} = V_{GB} - V_{FB} - \psi_{sm} - \gamma\sqrt{\psi_{am}},$$

(which decreases approximately exponentially with decreasing gate bias as the transistor drops out of strong inversion) the difference in surface potential between the drain and source is

(9) $$\Delta\psi_s = \psi_{sL} - \psi_{s0},$$

the bulk charge linearization factor is

(10) $$\alpha_m = 1 + \frac{\gamma}{2\sqrt{\psi_{am}}}\left(1 - e^{-\psi_{sm}/\phi_t}\right),$$

and

(11) $$H = \phi_t + \frac{\psi_{im}}{\alpha_m}.$$

Copyright © 2011 by Oxford University Press

All other symbols have the same meaning as in the book. These expressions are valid for all regions of operation, from accumulation through strong inversion.

For a specific bias condition $\psi_{s0} = \psi_{s0}(V_{GB}, V_{SB})$ and $\psi_{sL} = \psi_{sL}(V_{GB}, V_{DB})$, and several quantities above also depend on ψ_{s0} and ψ_{sL}, so the capacitance expressions will involve the derivative of these surface potentials with respect to the applied biases. One quantity that appears often in the derivation of the capacitances is

(12) $$\frac{\partial H}{\partial \psi_{sm}} = -\left[1 + \frac{\psi_{im}}{\alpha_m^2 \sqrt{\psi_{am}}}\left(\frac{\gamma e^{-\psi_{sm}/\phi_t}}{2\phi_t} - \frac{(\alpha_m - 1)^2}{\gamma}\right)\right]$$

and for compactness of notation the expressions below will be written in terms of that quantity.

Using $C_{ox} = WLC_{ox}^{'}$ we have, for $C_{mf} = -\partial Q_m / \partial V_f$,

(13) $$C_{gs} = \frac{C_{ox}}{2}\left(1 + \frac{\Delta\psi_s}{3H} + \frac{\Delta\psi_s^2}{12H^2}\frac{\partial H}{\partial \psi_{sm}}\right)\frac{\partial \psi_{s0}}{\partial V_{SB}}$$

(14) $$C_{gd} = \frac{C_{ox}}{2}\left(1 - \frac{\Delta\psi_s}{3H} + \frac{\Delta\psi_s^2}{12H^2}\frac{\partial H}{\partial \psi_{sm}}\right)\frac{\partial \psi_{sL}}{\partial V_{DB}}$$

(15) $$C_{gb} = C_{ox}\left[1 + \frac{\Delta\psi_s}{6H}\left(\frac{\partial \psi_{sL}}{\partial V_{GB}} + \frac{\partial \psi_{sL}}{\partial V_{DB}} - \frac{\partial \psi_{s0}}{\partial V_{GB}} - \frac{\partial \psi_{s0}}{\partial V_{SB}}\right) - \frac{1}{2}\left(1 + \frac{\Delta\psi_s^2}{12H^2}\frac{\partial H}{\partial \psi_{sm}}\right)\left(\frac{\partial \psi_{sL}}{\partial V_{GB}} + \frac{\partial \psi_{sL}}{\partial V_{DB}} + \frac{\partial \psi_{s0}}{\partial V_{GB}} + \frac{\partial \psi_{s0}}{\partial V_{SB}}\right)\right]$$

(16) $$C_{bs} = (\alpha_m - 1)C_{gs} - \left[\frac{\gamma e^{-\psi_{sm}/\phi_t}}{2\phi_t\sqrt{\psi_{am}}} - \frac{(\alpha_m - 1)^2}{\gamma\sqrt{\psi_{am}}}\right]\frac{\Delta\psi_s^2}{24H^2}\frac{\partial \psi_{s0}}{\partial V_{SB}}$$

(17) $$C_{bd} = (\alpha_m - 1)C_{gd} - \left[\frac{\gamma e^{-\psi_{sm}/\phi_t}}{2\phi_t\sqrt{\psi_{am}}} - \frac{(\alpha_m - 1)^2}{\gamma\sqrt{\psi_{am}}}\right]\frac{\Delta\psi_s^2}{24H^2}\frac{\partial \psi_{sL}}{\partial V_{DB}}$$

(18) $$C_{sd} = -\frac{C_{ox}}{4}\left\{\begin{matrix} \alpha_m + \dfrac{\Delta\psi_s}{6}\left[\dfrac{\gamma e^{-\psi_{sm}/\phi_t}}{2\phi_t\sqrt{\psi_{am}}} - \dfrac{(\alpha_m - 1)^2}{\gamma\sqrt{\psi_{am}}}\right]\left(\dfrac{\Delta\psi_s^2}{20H^2} + \dfrac{\Delta\psi_s}{2H} - 1\right) \\ -\dfrac{\alpha_m \Delta\psi_s^2}{12H^2}\left(\dfrac{\Delta\psi_s}{5H} + 1\right)\dfrac{\partial H}{\psi_{sm}} + \dfrac{\alpha_m}{3}\left(\dfrac{3\Delta\psi_s^2}{20H^2} - \dfrac{\Delta\psi_s}{H} - 1\right) \end{matrix}\right\}\frac{\partial \psi_{sL}}{\partial V_{DB}}.$$

The 3 other capacitive current elements in Fig. 8.5 involve the quantities

(19) $$C_m = C_{dg} - C_{gd}$$

(20) $$C_{mb} = C_{db} - C_{bd}$$

(21) $$C_{mx} = C_{bg} - C_{gb}$$

and these can be determined from the capacitances above with the 3 additional capacitances

Copyright © 2011 by Oxford University Press

$$C_{dg}=\frac{C_{ox}}{2}\left(\begin{array}{c}1-\frac{\Delta\psi_s^2}{12H^2}\left(\frac{\Delta\psi_s}{5H}+1\right)+\frac{\alpha_m}{6}\left(\frac{3\Delta\psi_s^2}{20H^2}+\frac{\Delta\psi_s}{H}-1\right)\left(\frac{\partial\psi_{sL}}{\partial V_{GB}}-\frac{\partial\psi_{s0}}{\partial V_{GB}}\right)\\ -\frac{1}{2}\left\{\alpha_m-\frac{\Delta\psi_s}{6}\left[\frac{\gamma e^{-\psi_{sm}/\phi_t}}{2\phi_t\sqrt{\psi_{am}}}-\frac{(\alpha_m-1)^2}{\gamma\sqrt{\psi_{am}}}\right]\left(\frac{\Delta\psi_s^2}{20H^2}+\frac{\Delta\psi_s}{2H}-1\right)+\frac{\alpha_m\Delta\psi_s^2}{12H^2}\left(\frac{\Delta\psi_s}{5H}+1\right)\frac{\partial H}{\partial\psi_{sm}}\right\}\left(\frac{\partial\psi_{sL}}{\partial V_{GB}}+\frac{\partial\psi_{s0}}{\partial V_{GB}}\right)\end{array}\right) \tag{22}$$

$$C_{db}=\frac{C_{ox}}{2}\left(\begin{array}{c}-1+\frac{\Delta\psi_s^2}{12H^2}\left(\frac{\Delta\psi_s}{5H}+1\right)-\frac{\alpha_m}{6}\left(\frac{3\Delta\psi_s^2}{20H^2}+\frac{\Delta\psi_s}{H}-1\right)\left(\frac{\partial\psi_{sL}}{\partial V_{GB}}+\frac{\partial\psi_{sL}}{\partial V_{DB}}-\frac{\partial\psi_{s0}}{\partial V_{GB}}-\frac{\partial\psi_{s0}}{\partial V_{SB}}\right)\\ +\frac{1}{2}\left\{\alpha_m-\frac{\Delta\psi_s}{6}\left[\frac{\gamma e^{-\psi_{sm}/\phi_t}}{2\phi_t\sqrt{\psi_{am}}}-\frac{(\alpha_m-1)^2}{\gamma\sqrt{\psi_{am}}}\right]\left(\frac{\Delta\psi_s^2}{20H^2}+\frac{\Delta\psi_s}{2H}-1\right)+\frac{\alpha_m\Delta\psi_s^2}{12H^2}\left(\frac{\Delta\psi_s}{5H}+1\right)\frac{\partial H}{\partial\psi_{sm}}\right\}\\ \times\left(\frac{\partial\psi_{sL}}{\partial V_{GB}}+\frac{\partial\psi_{sL}}{\partial V_{DB}}+\frac{\partial\psi_{s0}}{\partial V_{GB}}+\frac{\partial\psi_{s0}}{\partial V_{SB}}\right)\end{array}\right) \tag{23}$$

$$C_{bg}=C_{ox}\left(\begin{array}{c}\frac{(\alpha_m-1)\Delta\psi_s^2}{12\alpha_m H^2}-(\alpha_m-1)\frac{\Delta\psi_s}{6H}\left(\frac{\partial\psi_{sL}}{\partial V_{GB}}-\frac{\partial\psi_{s0}}{\partial V_{GB}}\right)\\ +\frac{1}{2}\left\{(\alpha_m-1)-\left[\frac{\gamma e^{-\psi_{sm}/\phi_t}}{2\phi_t\sqrt{\psi_{am}}}-\frac{(\alpha_m-1)^2}{\gamma\sqrt{\psi_{am}}}\right]\frac{\Delta\psi_s^2}{12H}+\frac{(\alpha_m-1)\Delta\psi_s^2}{12H^2}\frac{\partial H}{\partial\psi_{sm}}\right\}\left(\frac{\partial\psi_{sL}}{\partial V_{GB}}+\frac{\partial\psi_{s0}}{\partial V_{GB}}\right)\end{array}\right). \tag{24}$$

Approximations for Accumulation and Depletion Operation

In accumulation and depletion the inversion charge is negligible, and to a good approximation $\psi_{s0}=\psi_{sL}=\psi_{sm}=\psi_{sa}$ where ψ_{sa} is given by (3.2.24), and these depend only on V_{GB}; all derivatives of surface potential with respect to V_{SB} and V_{DB} are zero, and we also have $\Delta\psi_s=0$. We therefore directly get, from the capacitance expressions above,

$$C_{gs}=C_{gd}=C_{bs}=C_{bd}=C_{sd}=0\,. \tag{25}$$

The term involving V_{CB} in the surface potential equation (3.2.11), which represents the mobile electron concentration, can be ignored in accumulation and depletion, so we have

$$(V_{GB}-V_{FB}-\psi_s)^2=\gamma^2(\phi_t e^{-\psi_s/\phi_t}+\psi_s-\phi_t) \tag{26}$$

and implicitly differentiating this with respect to V_{GB}, and comparing to (7) and (10) gives

$$\frac{\partial\psi_s}{\partial V_{GB}}=\frac{V_{GB}-V_{FB}-\psi_s}{V_{GB}-V_{FB}-\psi_s+0.5\gamma^2(1-e^{-\psi_s/\phi_t})}=\frac{1}{\alpha_m}\,. \tag{27}$$

Using this, in addition to the information about the terms that go to zero, in (22) and (23), gives

$$C_{dg}=C_{db}=0\,. \tag{28}$$

Finally, from (15) and (24) we have, using (27),

$$C_{gb}=C_{bg}=C_{ox}\left(1-\frac{\partial\psi_s}{\partial V_{GB}}\right)=C_{ox}\left(1-\frac{1}{\alpha_m}\right) \tag{29}$$

therefore also $C_m=C_{mb}=C_{mx}=0$.

Copyright © 2011 by Oxford University Press

It could be intuitively expected that only C_{gb} and C_{bg} should be nonzero. In depletion and accumulation there is no inversion charge, so all derivatives of source and drain charges should be zero, and the source and drain regions cannot "communicate" with the MOS transistor and so cannot influence its behavior, therefore all derivatives with respect source and drain voltages should be zero. The charge balance within a MOS transistor then is between the gate charge and the bulk charge, the latter of which consists of depletion charge due to the ionized acceptor atoms and the accumulation charge due to mobile holes. The gate and bulk charges balance, and they vary with ψ_s, which is a function of V_{GB}, so C_{gb} should be nonzero. From Fig. 2.12 we see that as V_{GB} becomes increasingly negative below the flatband voltage, the derivative $\partial\psi_s/\partial V_{GB}$ starts at a positive value (which will be developed below) and monotonically decreases, asymptotically approaching zero for $V_{GB} \to -\infty$. C_{gb} therefore starts at a finite value less than C_{ox} at $V_{GB} = V_{FB}$ and asymptotically increases toward C_{ox} as V_{GB} becomes more negative, as Fig. 2.25 shows. Accurate modeling of capacitances around flatband is not important for MOS transistors, which are generally operated at higher values of V_{GB}, but is critical for modeling of MOS devices that are used as voltage variable capacitors [2][3][4][5].

The final expression in (29) in fact holds for all gate biases in the absence of inversion charge, and using (10) in (29) gives the high-frequency capacitance behavior curve of Fig. 2.25.

For operation in depletion somewhat above flatband, the $e^{-\psi_s/\phi_t}$ term, which relates to the accumulation component of charge, is negligible. Implicit differentiation of (2.5.4) gives $\partial\psi_s/\partial V_{GB} = 1/(1+0.5\gamma/\sqrt{\psi_s})$ and substituting this in (29) gives

$$(30) \qquad C_{gb} = C_{ox}\left(\frac{\gamma}{\gamma + 2\sqrt{\psi_{sa}}}\right) = C_{ox}\left(\frac{\gamma}{2\sqrt{\gamma^2/4 + V_{GB} - V_{FB}}}\right).$$

Note that (30) predicts that at $V_{GB} = V_{FB}$ we should have $C_{gb} = C_{ox}$, which is inaccurate; the gate-bulk capacitance, as we will see shortly, is less than C_{ox} at the flatband condition. Equation (30) is therefore only a reasonable approximation for operation where the $e^{-\psi_s/\phi_t}$ term in (3.2.11) (without the inversion charge component) is small compared to unity. Our analysis here in accumulation and depletion is based on the bulk charge model

$$(31) \qquad Q_B' = -\operatorname{sgn}(\psi_s)\sqrt{2q\varepsilon_s N_A}\sqrt{\phi_t e^{-\psi_s/\phi_t} + \psi_s - \phi_t}$$

which is valid in all regions of operation, yet the analysis leading to the definition of ψ_{sa} in the book is based on the simplified bulk charge model (2.6.7). This main seem contradictory, but is not; we are using the definition (2.5.5) of ψ_{sa} only to simplify the expressions.

For operation at flatband L'Hôpital's rule can be applied to (27), which results, after some manipulation, in

$$(32) \qquad \left.\frac{\partial\psi_s}{\partial V_{GB}}\right|_{V_{GB}=V_{FB}} = \frac{1}{1+\gamma/\sqrt{2\phi_t}}$$

and using this in (29) we have

$$(33) \qquad \left.C_{gb}\right|_{V_{GB}=V_{FB}} = C_{ox}\left(\frac{1}{1+\sqrt{2\phi_t}/\gamma}\right).$$

The gate-substrate capacitance is therefore less than C_{ox} at flatband, by an amount that depends on the gate dielectric thickness and substrate doping, which affect γ, and on the temperature, which affects ϕ_t.

In accumulation, the exponential term in the right hand side of (26) dominates. Keeping only this term and using the resulting approximation in (29) gives

Copyright © 2011 by Oxford University Press

(34) $$C_{gb} = C_{ox}\left(\frac{V_{GB} - V_{FB} - \psi_s}{V_{GB} - V_{FB} - \psi_s - 2\phi_t}\right) \approx C_{ox}\left(1 + \frac{2\phi_t}{V_{GB} - V_{FB} - \psi_s}\right).$$

In accumulation $V_{GB} - V_{FB} - \psi_s$ is negative, so as expected from our previous discussions C_{gb} will asymptotically increase towards the value C_{ox} as V_{GB} becomes more negative below flatband.

Approximations for Strong Inversion Nonsaturation Operation

In strong inversion nonsaturation operation, the source and drain surface potentials are approximately pinned to $\phi_0 + V_{SB}$ and $\phi_0 + V_{DB}$, respectively, and to first order do not depend on V_{GB}, so

(35) $$\frac{\partial \psi_{s0}}{\partial V_{SB}} = \frac{\partial \psi_{sL}}{\partial V_{DB}} = 1,$$

(36) $$\frac{\partial \psi_{s0}}{\partial V_{GB}} = \frac{\partial \psi_{sL}}{\partial V_{GB}} = 0,$$

(37) $$\Delta\psi_s = V_{DS}.$$

Additionally, the terms in $e^{-\psi_s/\phi_t}$, which relate to the accumulation holes, are negligible, and $\psi_{sm} >> \phi_t$. The quantities associated with the symmetric linearization charge sheet model therefore become, in terms of terminal voltages,

(38) $$\psi_{sm} = \phi_0 + 0.5(V_{SB} + V_{DB}) = \phi_0 + V_{SB} + 0.5V_{DS},$$

(39) $$\psi_{am} = \psi_{sm},$$

(40) $$\psi_{im} = V_{GB} - V_{FB} - \psi_{sm} - \gamma\sqrt{\psi_{sm}},$$

(41) $$\alpha_m = 1 + \frac{\gamma}{2\sqrt{\psi_{sm}}},$$

with H still given by (11) but with ψ_{im} from (40), and the derivative of H with respect to ψ_{sm}, (12), is

(42) $$\frac{\partial H}{\partial \psi_{sm}} = -\left(1 - \frac{(\alpha_m - 1)\psi_{im}}{2\alpha_m^2\psi_{sm}}\right).$$

Using these in the general capacitance expressions (13) through (24) gives

(43) $$C_{gs} = \frac{C_{ox}}{2}\left(1 + \frac{V_{DS}}{3H} + \frac{V_{DS}^2}{12H^2}\frac{\partial H}{\partial \psi_{sm}}\right)$$

(44) $$C_{gd} = \frac{C_{ox}}{2}\left(1 - \frac{V_{DS}}{3H} + \frac{V_{DS}^2}{12H^2}\frac{\partial H}{\partial \psi_{sm}}\right)$$

(45) $$C_{gb} = -C_{ox}\frac{V_{DS}^2}{12H^2}\frac{\partial H}{\partial \psi_{sm}}$$

Copyright © 2011 by Oxford University Press

(46) $$C_{bs} = (\alpha_m - 1)C_{gs} + \frac{(\alpha_m - 1)^2}{\gamma\sqrt{\psi_{am}}}\frac{V_{DS}^2}{24H^2}$$

(47) $$C_{bd} = (\alpha_m - 1)C_{gd} + \frac{(\alpha_m - 1)^2}{\gamma\sqrt{\psi_{am}}}\frac{V_{DS}^2}{24H^2}$$

(48) $$C_{sd} = -\frac{C_{ox}}{4}\left(\alpha_m - \frac{V_{DS}}{6}\frac{(\alpha_m - 1)^2}{\gamma\sqrt{\psi_{am}}}\left(\frac{V_{DS}^2}{20H^2} + \frac{V_{DS}}{2H} - 1\right) + \frac{\alpha_m}{6}\left(\frac{3V_{DS}^2}{20H^2} - \frac{V_{DS}}{H} - 1\right) - \frac{\alpha_m V_{DS}^2}{12H^2}\left(\frac{V_{DS}}{5H} + 1\right)\frac{\partial H}{\partial \psi_{sm}}\right)$$

(49) $$C_{dg} = \frac{C_{ox}}{2}\left(1 - \frac{V_{DS}^2}{12H^2}\left(\frac{V_{DS}}{5H} + 1\right)\right)$$

(50) $$C_{db} = \frac{C_{ox}}{2}\left(\alpha_m - 1 + \frac{V_{DS}^2}{12H^2}\left(\frac{V_{DS}}{5H} + 1\right) + \frac{V_{DS}}{6}\left(\frac{(\alpha_m - 1)^2}{\gamma\sqrt{\psi_{am}}}\right)\left(\frac{V_{DS}^2}{20H^2} + \frac{V_{DS}}{2H} - 1\right) + \frac{\alpha_m V_{DS}^2}{12H^2}\left(\frac{V_{DS}}{5H} + 1\right)\frac{\partial H}{\partial \psi_{sm}}\right)$$

(51) $$C_{bg} = C_{ox}\left(\frac{(\alpha_m - 1)V_{DS}^2}{12\alpha_m H^2}\right).$$

Although these expressions depend on H and $\partial H/\partial \psi_{sm}$, which in turn depend on V_{DS}, V_{GB}, and V_{SB}, they give explicit formulas for the capacitances from the symmetric linearization charge sheet model in strong inversion nonsaturation.

In contrast to the general expressions for $V_{DS} = 0$, that we will derive below, which predict a small positive value for C_{gb} and C_{bg} under that bias condition, in deriving the strong inversion approximations we have ignored the small variation of surface potential with gate voltage, which is why (45) and (51) predict that $C_{gb} = C_{bg} = 0$ for $V_{DS} = 0$. Careful inspection of Fig. 1 and Fig. 2, below, show the slight nonzero value at $V_{DS} = 0$. Similarly, (43) and (44) predict that at $V_{DS} = 0$ we should have $C_{gs} = C_{gd} = C_{ox}/2$; Fig. 1 shows that these capacitances are in fact slightly smaller than $C_{ox}/2$; this is because the surface potentials are not exactly pinned to $\phi_0 + V_{SB}$ and $\phi_0 + V_{DB}$ in strong inversion.

Approximations for Strong Inversion Saturation Operation

There is no abrupt transition at saturation, rather as V_{DS} increases the drain end of the channel gradually drops out of strong inversion, and will eventually enter weak inversion for sufficiently large drain bias. At this point, using the weak inversion analysis of Sec. 2.6.3, we have

(52) $$\psi_{sL} = \psi_{sa}$$

where ψ_{sa} is given by (2.6.27),

(53) $$\frac{\partial \psi_{sL}}{\partial V_{DB}} = 0,$$

(54) $$\frac{\partial \psi_{sL}}{\partial V_{GB}} = 1 + \frac{\gamma}{2\sqrt{\psi_{sa}}}$$

and we will still have $\psi_{s0} = \phi_0 + V_{CB}$, $\partial \psi_{s0}/\partial V_{SB} = 1$, and $\partial \psi_{s0}/\partial V_{GB} = 0$. The difference between the drain and source surface potentials is then

(55) $$\Delta\psi_s = \psi_{sa} - \phi_0 - V_{SB},$$

Copyright © 2011 by Oxford University Press

the midpoint surface potential is

(56) $$\psi_{sm} = \frac{\phi_0 + V_{SB} + \psi_{sa}}{2},$$

and (39) through (42) are still valid with ψ_{sm} from (56). Using these simplifications in (13) through (24) gives

(57) $$C_{gs} = \frac{C_{ox}}{2}\left(1 + \frac{\Delta\psi_s}{3H} + \frac{\Delta\psi_s^2}{12H^2}\frac{\partial H}{\partial \psi_{sm}}\right)$$

(58) $$C_{gd} = 0$$

(59) $$C_{gb} = C_{ox}\left(1 + \frac{\Delta\psi_s}{12H}\frac{\gamma}{\sqrt{\psi_{sa}}} - \left(1 + \frac{\Delta\psi_s^2}{12H^2}\frac{\partial H}{\partial \psi_{sm}}\right)\left(1 + \frac{\gamma}{4\sqrt{\psi_{sa}}}\right)\right)$$

(60) $$C_{bs} = (\alpha_m - 1)C_{gs} + \frac{(\alpha_m - 1)^2}{\gamma\sqrt{\psi_{am}}}\frac{\Delta\psi_s^2}{24H^2}$$

(61) $$C_{bd} = 0$$

(62) $$C_{sd} = 0$$

(63) $$C_{dg} = \frac{C_{ox}}{2}\left\{\begin{array}{c} 1 - \frac{\Delta\psi_s^2}{12H^2}\left(\frac{\Delta\psi_s}{5H} + 1\right) + \frac{\alpha_m}{6}\left(\frac{3\Delta\psi_s^2}{20H^2} + \frac{\Delta\psi_s}{H}\right)\left(1 + \frac{\gamma}{2\sqrt{\psi_{sa}}}\right) \\ -\left[\frac{2\alpha_m}{3} + \frac{\Delta\psi_s}{12}\frac{(\alpha_m - 1)^2}{\gamma\sqrt{\psi_{am}}}\left(\frac{\Delta\psi_s^2}{20H^2} + \frac{\Delta\psi_s}{2H} - 1\right) + \frac{\alpha_m\Delta\psi_s^2}{24H^2}\left(\frac{\Delta\psi_s}{5H} + 1\right)\frac{\partial H}{\partial \psi_{sm}}\right]\left(1 + \frac{\gamma}{2\sqrt{\psi_{sa}}}\right) \end{array}\right\}$$

(64) $$C_{db} = \frac{C_{ox}}{2}\left\{\begin{array}{c} -1 + \frac{\Delta\psi_s^2}{12H^2}\left(\frac{\Delta\psi_s}{5H} + 1\right) - \frac{\alpha_m}{3}\left(\frac{3\Delta\psi_s^2}{20H^2} + \frac{\Delta\psi_s}{H}\right)\left(1 + \frac{\gamma}{4\sqrt{\psi_{sa}}}\right) \\ +\left[\frac{4\alpha_m}{3} + \frac{\Delta\psi_s}{6}\frac{(\alpha_m - 1)^2}{\gamma\sqrt{\psi_{am}}}\left(\frac{\Delta\psi_s^2}{20H^2} + \frac{\Delta\psi_s}{2H} - 1\right) + \frac{\alpha_m\Delta\psi_s^2}{12H^2}\left(\frac{\Delta\psi_s}{5H} + 1\right)\frac{\partial H}{\partial \psi_{sm}}\right]\left(1 + \frac{\gamma}{4\sqrt{\psi_{sa}}}\right) \end{array}\right\}$$

(65) $$C_{bg} = C_{ox}\left\{\frac{(\alpha_m - 1)\Delta\psi_s^2}{12\alpha_m H^2} + \frac{1}{2}\left[(\alpha_m - 1)\left(1 - \frac{\Delta\psi_s}{3H}\right) + \frac{(\alpha_m - 1)^2}{\gamma\sqrt{\psi_{am}}}\frac{\Delta\psi_s^2}{12H} + \frac{(\alpha_m - 1)\Delta\psi_s^2}{12H^2}\frac{\partial H}{\partial \psi_{sm}}\right]\left(1 + \frac{\gamma}{2\sqrt{\psi_{sa}}}\right)\right\}.$$

Exact Capacitances for V_{ds}=0

If $V_{DS} = 0$ we have $\psi_{s0} = \psi_{sL} = \psi_{sm} = \psi_s$, so $\Delta\psi_s = 0$, and $\partial\psi_{s0}/\partial V_{GB} = \partial\psi_{sL}/\partial V_{GB} = \partial\psi_s/\partial V_{GB}$. The total capacitance at the gate terminal C_{gg} is, summing (13), (14), and (15),

(66) $$C_{gg} = C_{gs} + C_{gd} + C_{gb} = C_{ox}\left(1 - \frac{\partial\psi_s}{\partial V_{GB}}\right).$$

Copyright © 2011 by Oxford University Press

This result is general and holds for $V_{DS}=0$ for all regions of operation. Implicit differentiation of the surface potential equation (3.2.11) gives (Prob. 3.18), without simplification for a specific region of operation,

(67) $$\frac{\partial \psi_s}{\partial V_{GB}} = \frac{V_{GB} - V_{FB} - \psi_s}{V_{GB} - V_{FB} - \psi_s + 0.5\gamma^2\left(1 - e^{-\psi_s/\phi_t} + e^{-(2\phi_F + V_{CB})/\phi_t}(e^{\psi_s/\phi_t} - 1)\right)}.$$

As ψ_s becomes less the zero, i.e. for operation in accumulation, the $e^{-\psi_s/\phi_t}$ term in the denominator of this expression becomes large and $\partial\psi/V_{GB}$ approaches zero. Similarly, for $\psi_s >> 2\phi_F + V_{CB}$, i.e. for operation in strong inversion, the e^{ψ_s/ϕ_t} term in the denominator of this expression becomes large and $\partial\psi/V_{GB}$ again approaches zero. Hence C_{gg} will asymptotically approach C_{ox} in both accumulation and strong inversion. Using the relations (66) and (67) gives the low-frequency behavior capacitance curve (solid line) of Fig. 2.25.

The capacitances (13) through (24) simplify to

(68) $$C_{gs} = C_{gd} = \frac{C_{ox}}{2}\frac{\partial \psi_s}{\partial V_{CB}}$$

(69) $$C_{gb} = C_{ox}\left(1 - \left(\frac{\partial \psi_s}{\partial V_{GB}} + \frac{\partial \psi_s}{\partial V_{CB}}\right)\right)$$

(70) $$C_{bs} = C_{bd} = (\alpha_m - 1)\frac{C_{ox}}{2}\frac{\partial \psi_s}{\partial V_{CB}}$$

(71) $$C_{sd} = C_{ox}\left(-\frac{\alpha_m}{6}\frac{\partial \psi_s}{\partial V_{DB}}\right)$$

(72) $$C_{dg} = \frac{C_{ox}}{2}\left(1 - \alpha_m\frac{\partial \psi_s}{\partial V_{GB}}\right)$$

(73) $$C_{db} = \frac{C_{ox}}{2}\left(\alpha_m\left(\frac{\partial \psi_s}{\partial V_{GB}} + \frac{\partial \psi_s}{\partial V_{CB}}\right) - 1\right)$$

(74) $$C_{bg} = C_{ox}\left((\alpha_m - 1)\frac{\partial \psi_s}{\partial V_{GB}}\right)$$

(75) $$C_{mx} = 2C_{mb} = -2C_m = C_{ox}\left[\left(\alpha_m\frac{\partial \psi_s}{\partial V_{GB}} + \frac{\partial \psi_s}{\partial V_{CB}}\right) - 1\right].$$

This last expression shows that the body-referenced all-region has a small non-reciprocity in capacitances at $V_{DS}=0$.

In strong inversion $\partial\psi_s/\partial V_{GB}$ is not exactly equal to zero, it has a small positive value, and $\partial\psi_s/\partial V_{CB}$ is not exactly 1, it is slightly less. The magnitude of the capacitances in (75) therefore falls off rather slowly, approximately inversely with increasing gate voltage, in strong inversion. As the gate voltage decreases and operation transitions to weak inversion, depletion, and accumulation, $\partial\psi_s/\partial V_{CB}$ approaches zero and from (27) $\partial\psi_s/\partial V_{GB}$ approaches $1/\alpha_m$, therefore the amount of non-reciprocity approaches zero (it does so very rapidly as the gate voltage is reduced, because the inversion charge decreases approximately exponentially with gate voltage in weak inversion).

This nonreciprocal behavior, even at $V_{DS}=0$, is a consequence of the charge sheet approximation [6]; TCAD simulation and the Pao-Sah model [7], which is the reference for all MOSFET models (but involves double integrals and is requires numerical solution, so is not suitable for analytic or circuit simulation models), satisfy reciprocity at $V_{DS}=0$. The

Copyright © 2011 by Oxford University Press

amount of non-reciprocity is small, and has not proven to cause problems for circuit design. The above formula (75) quantifies the degree of non-reciprocity in the body-referenced all-region model based on symmetric linearization.

For the case of strong inversion where $V_{DS} = 0$, the source and drain surface potentials are approximately pinned to $\phi_0 + V_{SB}$ and $\phi_0 + V_{DB}$, respectively, and to first order do not depend on V_{GB}, so (35) through (37) hold and we have

(76) $$C_{gs} = C_{gd} = C_{dg} = \frac{C_{ox}}{2}$$

(77) $$C_{gb} = C_{bg} = 0$$

(78) $$C_{bs} = C_{bd} = C_{db} = (\alpha_m - 1)\frac{C_{ox}}{2} = C_{ox}\frac{\gamma}{2\sqrt{\phi_0 + V_{CB})}}$$

(79) $$C_{sd} = -\frac{\alpha_m}{6}C_{ox}$$

therefore also $C_m = C_{mb} = C_{mx} = 0$.

Copyright © 2011 by Oxford University Press

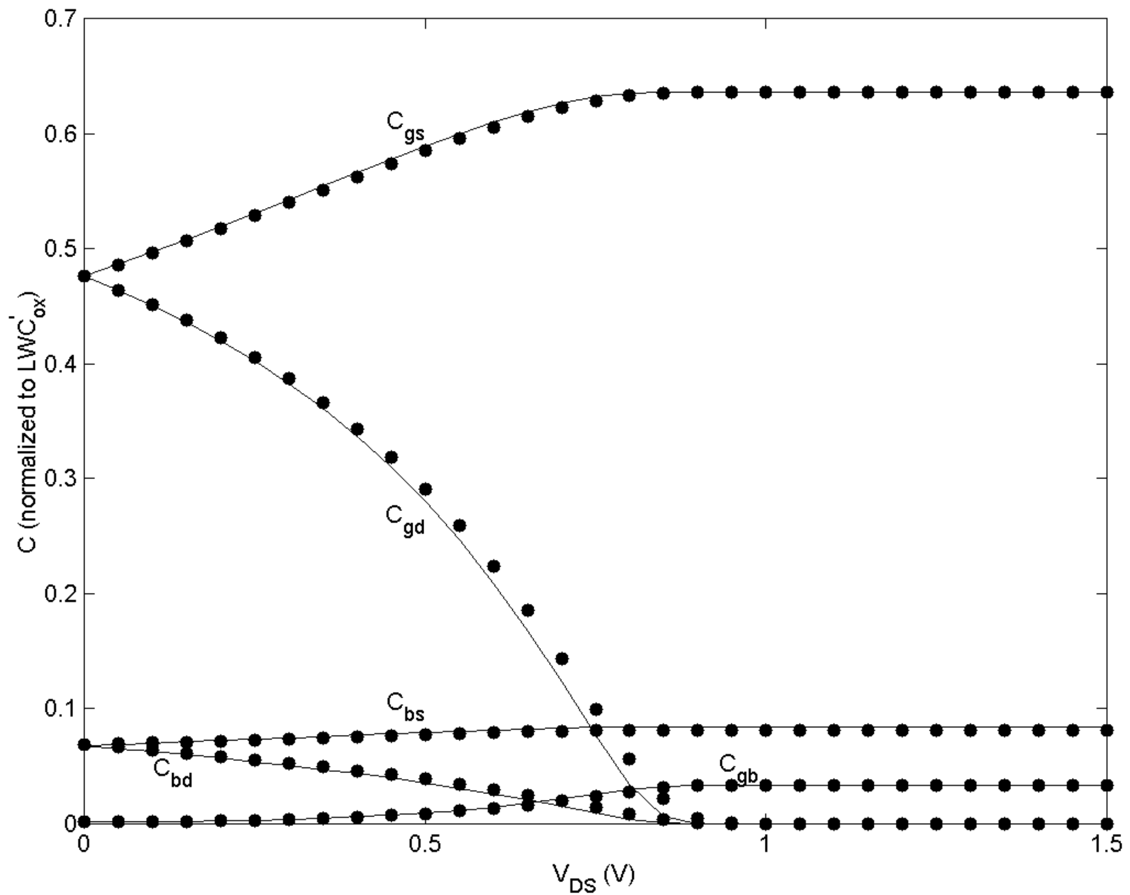

Fig. 1 Capacitances for the medium frequency small-signal model of Chap 7, for the complete all-region model (lines) and the body-referenced all-region symmetric linearization model (symbols). W/L=10µm/10µm, V_{FB} =-0.8, N_A=5×10^{17}cm^{-3}, t_{ox}=25Å, V_{SB}=0, and V_{GB}=1.4V. This is for operation in strong inversion; the complete all-region model is not valid in accumulation or the bottom of depletion.

Copyright © 2011 by Oxford University Press

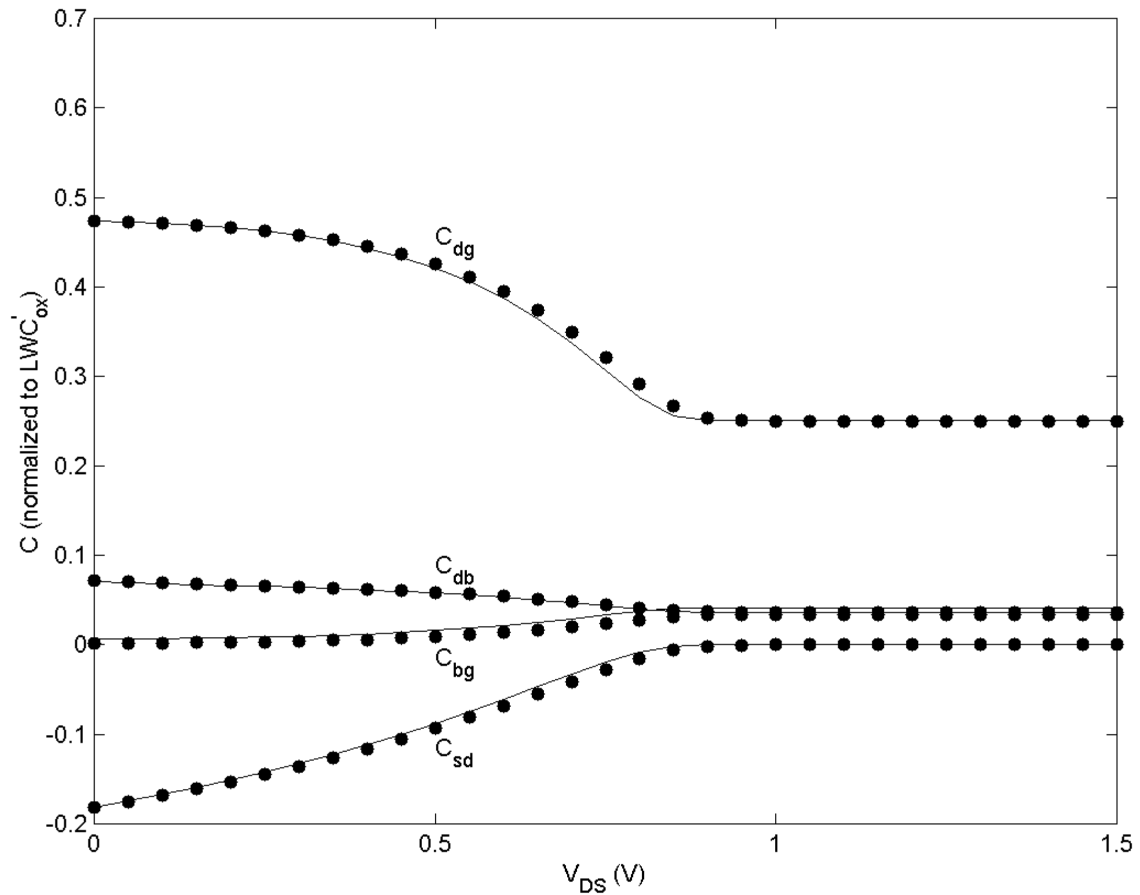

Fig. 2 Additional capacitances for the high frequency small-signal model of Chap 8, for the complete all-region model (lines) and the body-referenced all-region symmetric linearization model (symbols). W/L=10μm/10μm, V_{FB} =-0.8, N_A=5×10^{17}cm^{-3}, t_{ox}=25Å, V_{SB}=0, and V_{GB}=1.4V. This is for operation in strong inversion; the complete all-region model is not valid in accumulation or the bottom of depletion.

Copyright © 2011 by Oxford University Press

References

[1] G. Gildenblat, W. Wu, X. Li, R. van Langevelde, A. J. Scholten, G. D. J. Smit, and D. B. M. Klaassen, "Surface-potential-based compact model of bulk MOSFET," in *Compact Modeling: Principles, Techniques and Applications*, G. Gildenblat (Ed), Springer, pp. 3-40, 2010.

[2] F. Svelto, P. Erratico, S. Manzini, and R. Castello, "A metal-oxide-semiconductor varactor," *IEEE Electron Device Letters*, vol. 20, no. 3, pp. 164-166, March 1999.

[3] S. Pavan, Y. Tsividis, and K. Nagaraj, "Modeling of accumulation MOS capacitors for analog design in digital VLSI processes," *Proceedings of the International Conference on Circuits and Systems*, pp. 202-205, May 1999.

[4] A. Porret, T. Melly, C. C. Enz, and E. A. Vittoz, "Design of high-Q varactors for low-power wireless applications using a standard CMOS process," *IEEE Journal of Solid-State Circuits*, vol. 35, no. 3, pp. 337-345, March 2000.

[5] P. Andreani and S. Mattisson, "On the use of MOS varactors in RF VCO's," *IEEE Journal of Solid-State Circuits*, vol. 35, no. 6, pp. 905-910, June 2000.

[6] R. van Langevelde, A. J. Scholten, and D. B. M. Klaassen, "Physical background of MOS model 11," Philips Nat. Lab. Unclassified Report NL-UR 2003/00239, April 2003 [Online]: http://www.nxp.com/models/mos_models/model11/index.html

[7] H. C. Pao and C.-T. Sah, "Effects of diffusion current on characteristics of metal-oxide (insulator) semiconductor transistors," *Solid-State Electronics*, vol. 9, no. 10, pp. 927-937, 1966.

Copyright © 2011 by Oxford University Press

Capacitance is the ratio of the amount of electric charge stored on a conductor to a difference in electric potential. There are two closely related notions of capacitance: self capacitance and mutual capacitance.:237â€“238 Any object that can be electrically charged exhibits self capacitance. In this case the electric potential difference is measured between the object and ground. A material with a large self capacitance holds more electric charge at a given potential difference than one with low This capacitance is present due to the capacitive coupling from the gate metal to the source/drain contact metal vias as shown in Fig. 5.9. The outer fringe capacitance [9] is modeled as an equivalent parallel plate capacitor with the capacitance per unit width controlled by the fitting parameters CFS and CFD at the source and at the drain side, respectively. The charge associated with the outer fringe capacitance for capacitance between the gate and the source is modeled as. Figure 5.9.Â Capacitance. Reference. Chemically modified graphene. 130 F gâˆ’1.Â It is also notable that the Î´C after the aging is almost consistent for the two specimens. In other words, the aging in the second stage could be moved to the first stage by firing in air atmosphere. This survey focuses on linear, surface-based algorithms for mesh deformation. We address surface-based techniques, as opposed to space deformations or free-form deformations, since currently there is no comprehensive survey that reviews the former, while space-deformations are well exposed in the literature (see, e.g., [6], [46]).Â The linearization will be shown to distort ne-scale geometric details, which is taken care of by mul-tiresolution deformations (Section II-D).Â In comparison to FEM, a discretization based on nite differences is considerably easier to use, in particular since the Euler-Lagrange equations (4) only require a discretization of the Laplace-Beltrami operator.